Carbohydrate Polymers 84 (2011) 1426–1429

Contents lists available at ScienceDirect

Carbohydrate Polymers

journal homepage: www.elsevier.com/locate/carbpol

Short communication

Amylose wrapped halloysite nanotubes

Peter R. Chang [a], Yanfang Xie [b], Dongliang Wu [b], Xiaofei Ma [b,*]

[a] Bioproducts and Bioprocesses National Science Program, Agriculture and Agri-Food Canada, 107 Science Place, Saskatoon, SK, S7N 0X2, Canada
[b] School of Science, Tianjin University, Tianjin 300072, China

ARTICLE INFO

Article history:
Received 22 November 2010
Received in revised form 16 January 2011
Accepted 21 January 2011
Available online 28 January 2011

Keywords:
Halloysite nanotubes
Amylose
Supramolecular structure

ABSTRACT

Amylose was isolated from starch-rich yam, *Dioscorea opposita* Thunb. and used to prepare a halloysite nanotubes (HNTs) supramolecular structure by mechanical force. The thus obtained amylose wrapped halloysite nanotubes (amylose-HNTs) were characterized subsequently. Transmission electron microscopy and thermogravimetric analysis showed that the walls of the HNTs were wrapped with an amylose component (about 44.1 wt%). FTIR indicated that structural changes to amylose were related to the C–O–C groups of amylose in the interaction between amylose and the outer surface of the HNTs. Good dispersion of amylose-HNT in the DMSO/H_2O solution also illustrated that an interaction existed between amylose and the HNT outer surface.

1. Introduction

Halloysite is an aluminosilicate clay mineral that has a predominantly hollow nanotube structure with an inner diameter of 10–150 nm. Halloysite is formed naturally by surface weathering of minerals on Earth and has been used in nanocomposites, nanocontainers, and adsorbents (Wang et al., 2010). Halloysite nanotube (HNT) is an economical alternative to carbon nanotube that can be simply mined from the corresponding deposit (Shchukin, Sukhorukov, Price, & Lvov, 2005). HNTs have a wide variety of biological and non-biological applications; they have been used for storing molecular hydrogen, for catalytic conversions and processing of hydrocarbons, for removing environmental hazardous species, as a diuretic drug delivery (Shamsi & Geckeler, 2008), and as enzymatic nanoreactors (Shchukin et al., 2005). Recently much of the effort in the development of efficient and facile methods of dispersing carbon nanotubes (CNTs) in aqueous media has been focused on non-covalent functionalization of CNT surfaces (Alpatova et al., 2010). Dispersion via non-covalent functionalization is based on direct contact between a CNT and a biomolecule and many biomolecules such as proteins (Karajanagi et al., 2006), DNA (Enyashin, Gemming, & Seifert, 2007), amylose (Kim et al., 2004) or starch (Star, Steuerman, Heath, & Stoddart, 2002) and Gum Arabic (Bandyopadhyaya, Nativ-Roth, Regev, & Yerushalmi-Rozen, 2002) have been researched as dispersants for CNTs. There are few studies, however, on non-covalent functionalization of HNTs with biomolecules to improve the biocompatibility of HNTs. In the paper, we report a facile and green method for preparing a supramolecular complex of amylose and HNT in solid state using just mechanical force. This work also emphasizing on the structure of thus prepared amylose-wrapped HNTs (amylose-HNT) in terms of morphology, FTIR, thermal stability, and dispersion in solution.

2. Materials and methods

2.1. Materials

Dioscorea opposita Thunb. was obtained from Henan province, China. The HNTs were obtained from Hunan province, China. Ethanol and dimethyl sulfoxide (DMSO) were of analytical grade from Tianjin Chemical Reagent Factory, China.

2.2. Isolation of starch and amylose

Starch was isolated from *D. opposita* Thunb. according to the method of Xie, Chang, Wang, Yu, and Ma (2011). Amylose from *D. opposita* Thunb. starch was purified using Schoch's butanol precipitation method (Schoch, 1942).

2.3. Preparation of amylose-wrapped HNT

Equal amounts of HNT and amylose (50 mg) were placed in a ball milling apparatus and the mixture was milled for 20 min at room temperature. A very fine, homogeneous, pale-white powder was obtained, and was thoroughly dispersed in a 3/2 (w/w) DMSO/water solution by shaking. The solution was allowed to stand for 24 h to precipitate unwrapped HNTs and remove the free amy-

* *Corresponding author*. Tel.: +86 22 27406144; fax: +86 22 27403475.
E-mail address: maxiaofei@tju.edu.cn (X. Ma).

0144-8617/$ – see front matter.
doi:10.1016/j.carbpol.2011.01.038

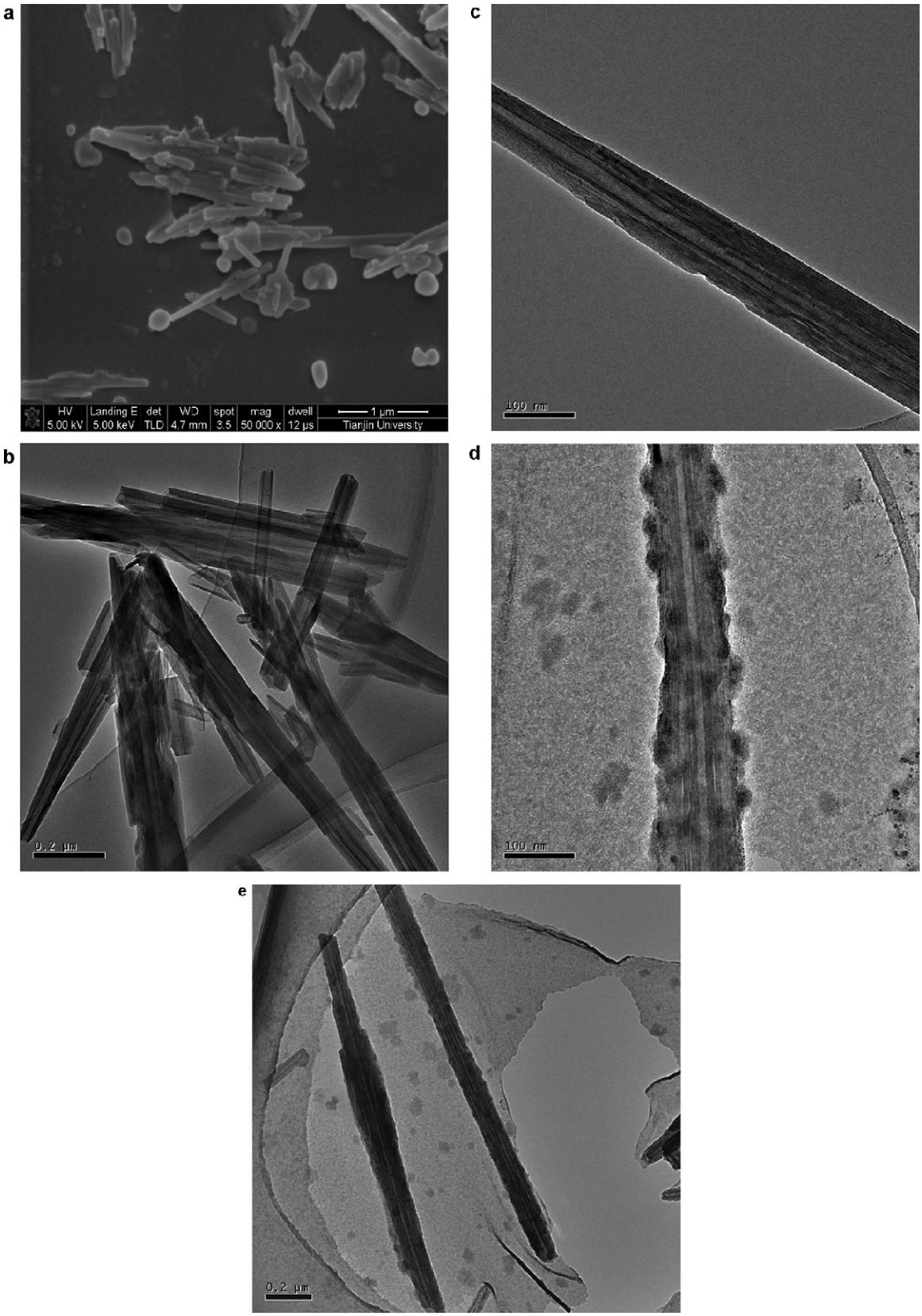

Fig. 1. SEM of HNTs (a), TEM of amylose (b and c), and TEM of amylose-HNT (d and e).

lose. The supernatant products were collected. In order to obtain precipitated products, ethanol was added to the supernatant. The product was then obtained by filtration, and washed with ethanol and then dried in a vacuum oven at 40 °C for 4 h.

2.4. Characterization

Scanning electron microscopy (SEM) images were obtained using a Philips XL-3 field emission scanning electron microscope.

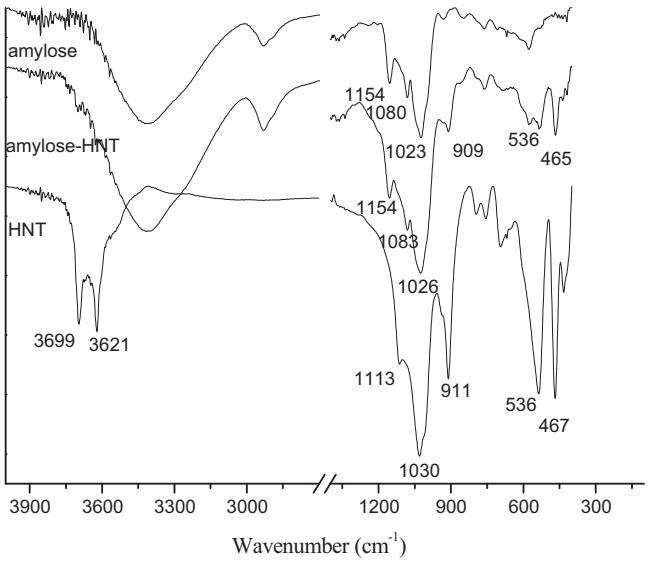

Fig. 2. FTIR spectra of HNT, amylose-HNT, and amylose.

Transmission electron microscopy (TEM) images were obtained with a JEM-2100, and the samples were prepared by placing a few drops on a mesh copper grid before examination. FTIR spectra were performed at 2 cm^{-1} resolution on a BIO-RAD FTS3000 IR Spectrum Scanner. Samples were prepared by making pellets with dried IR grade KBr, and typically, 64 scans were signal-averaged to reduce spectral noise. The thermal properties of amylose and amylose-HNT were measured with a ZTY-ZP type thermal analyzer. Sample weights varied from 5 to 10 mg, and they were heated in Al_2O_3 pans from room temperature to 600 °C at a heating rate of 15 °C/min in a nitrogen atmosphere with a flow rate of 30 mL/min.

3. Results and discussion

As revealed in Fig. 1(a), HNTs exhibited an agglomeration of nanotubes with a size of 10–100 nm in diameter and about 1–2 μm in length. The TEM image of HNTs (Fig. 1(b) and (c)) shows the layered walls and a hollow cavity of about 10–20 nm in diameter. When HNT and amylose were milled, the mechanical force wrapped helical amylose around the walls of HNTs. The pristine HNTs showed a smooth surface in Fig. 1(c), while the surface of HNT-amylose was rough (Fig. 1(d) and (e)). HNT-amylose exhibited the obvious core–shell structure.

Fig. 2 shows the FTIR spectra of HNT, amylose, and HNT-amylose. In the fingerprint region of the amylose spectrum, there are three peaks that are characteristic of –C–O– stretching. The peak at 1154 cm^{-1} was ascribed to C–O bond stretching of the C–O–H group, and the peaks at 1080 and 1023 cm^{-1} were attributed to C–O bond stretching of the C–O–C group in the anhydroglucose ring (Ma, Chang, Yang, & Yu, 2009). The HNT-amylose sample showed some signals due to HNT, such as the deformations of Al–O–Si and Si–O–Si at 536 and 462 cm^{-1}, respectively, and the O–H deformation of the inner hydroxyl groups at 909 cm^{-1}. In the HNT spectrum, the band at 1030 cm^{-1} was assigned to perpendicular Si–O stretching and at 1113 cm^{-1} to the apical Si–O vibration (Tierrablanca, Romero-García, Roman, & Cruz-Silva, 2010). In the HNT-amylose spectrum, these two bands may be overlapped with the peaks of C–O bond stretching at 1080 and 1023 cm^{-1}. The peak at 1154 cm^{-1} in amylose appeared without a shift, while the 1080 and 1023 cm^{-1} bands shifted to 1083 and 1026 cm^{-1}. This result indicated that the structural changes of amylose were related to the amylose C–O–C groups in the interaction between amylose and the outer surface of the nanotubes, when the amylose helix wrapped around HNT. This was similar to the DNA-wrapped HNTs (Shamsi & Geckeler, 2008). The absorptions bands at 3699 and 3621 cm^{-1} in the FTIR spectrum of HNT were respectively assigned to the stretching vibration due to external and internal O–H groups of HNT (Nicolini, Fukamachi, Wypych, & Mangrich, 2009). However, these bands could not be observed in the FTIR spectrum of amylose-HNT. When the external hydroxyl groups of HNTs formed the interactions with C–O–C groups of amylose, the band at 3699 cm^{-1} could shift blue (Nicolini et al., 2009). Therefore, it was possible that they were overlapped with the band at 3420 cm^{-1}, ascribed to hydrogen-bonded hydroxyl groups of amylose.

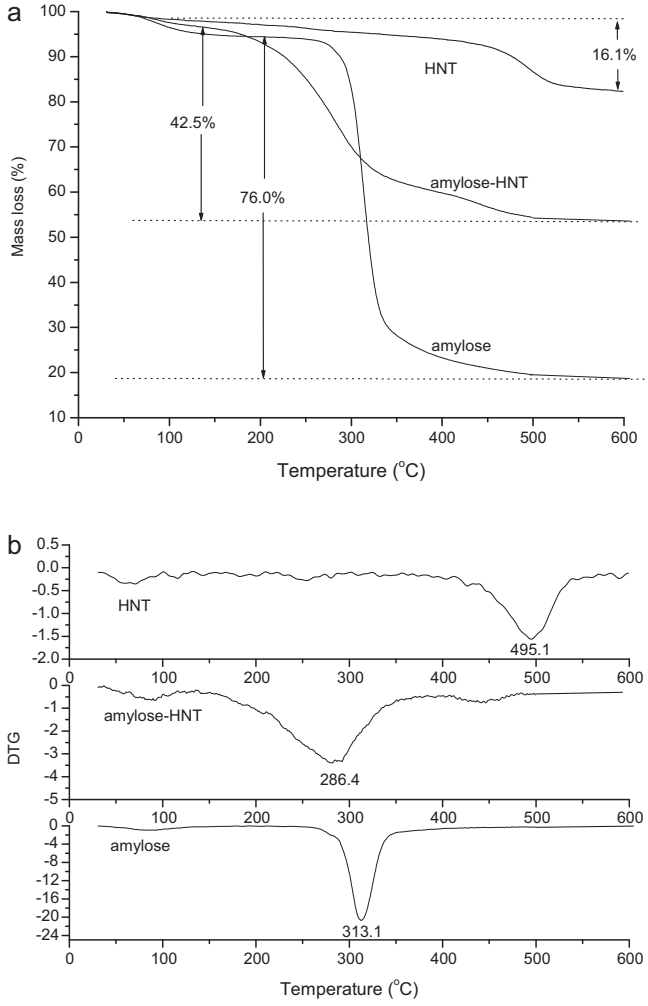

Fig. 3. TG (a) and DTG (b) curves of HNT, amylose, and amylose-HNT.

The thermogravimetric (TG) and derivative thermogravimetric (DTG) curves of the amylose, HNT, and amylose-HNT are shown in Fig. 3. As revealed by the DTG curves, amylose and HNT exhibited peaks at about 313.1 and 495.1 °C, respectively, i.e. the temperature at maximum rate of mass loss. The mass loss before the onset temperature was related to the volatilization of water contained in the amylose (Chang, Jian, Yu, & Ma, 2010). The temperature range where the peak of the DTG curves was located was the decomposition temperature of amylose. HNTs showed an initial weight loss due to residual water and a major weight loss at 495.1 °C which was assigned to the dehydroxylation of structural aluminol groups present in HNTs (Peng et al., 2008). It was assumed that the contents of mass loss of amylose and HNT, as revealed by TG curves, were constant in the decomposition temperature range when HNTs

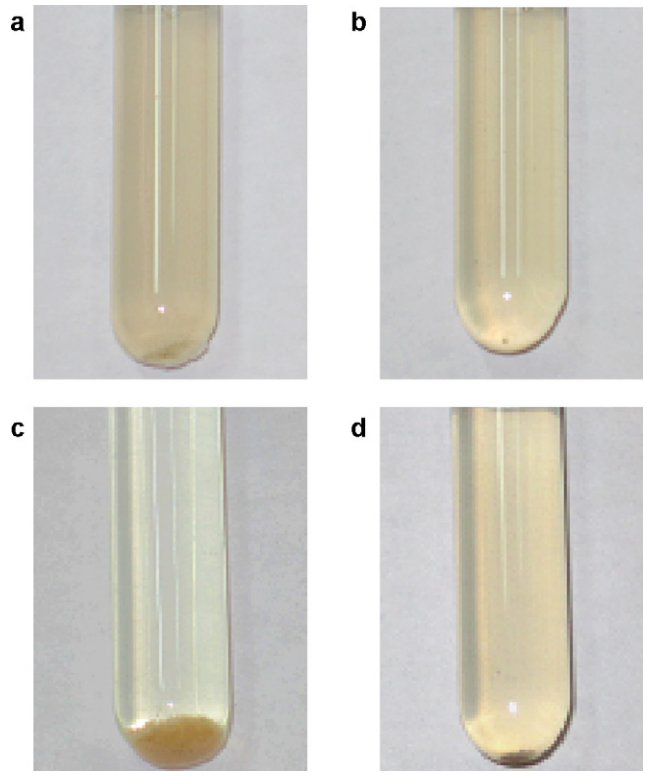

Fig. 4. Photographs of the dispersions of HNT (a and c) and amylose-HNT (b and d) in DMSO/H_2O solution at 0 h (a and b) and 24 h (c and d).

formed the complex with amylose. The content of amylose (w) in HNT-amylose could be calculated according to following equation:

$$1 \times w \times \alpha_1 + 1 \times (1 - w) \times \alpha_2 = 1 \times \alpha_3$$

where α_1 is the mass loss of amylose (76.0%) at 313.1 °C; α_2 is the mass loss of HNTs (16.1%) at 495.1 °C; α_3 is the mass loss of amylose (42.5%) at 286.4 °C. Therefore, the content of amylose (w) in amylose-HNT was estimated to be about 44.1%; the HNT content was 55.9%.

The dispersions of HNT (about 2 mg ml^{-1}) and amylose-HNT (about 4 mg ml^{-1}) in DMSO/H_2O solution are displayed in Fig. 4. The HNT and amylose-HNT were respectively added to DMSO/H_2O solution and the mixtures shaken on a rotary shaker at 150 rpm for 5 min. The HNT and amylose-HNT DMSO/H_2O dispersions were studied with the storage time (at 0 and 24 h). In Fig. 4(a), precipitation of HNT was observed at 0 h due to the high density and the long tubular structure of HNTs (Shamsi & Geckeler, 2008). Because DMSO/H_2O solution was a good dispersant for amylose, the amylose-HNT dispersed well in the solution (as shown in Fig. 4(b)), and no obvious precipitation was found. After the suspensions were stored for 24 h, the HNTs were completely precipitated from the solution and the solution was clear (as shown in Fig. 4(c)). In contrast, only a small amount of HNT precipitation was observed and the solution was not transparent in Fig. 4(d). Over the test storage period of two weeks, no more HNTs precipitated from the solution and the stability was maintained. This was probably dependent on the interactions between amylose and the outer surface of the HNTs.

4. Conclusions

Amylose was wrapped onto the surface of the HNTs to improve the biocompatibility of HNTs. The amylose component (about 44.1 wt%) assisted in the dispersion of amylose-HNTs in solution due to the supramolecular interaction between the C–O–C groups of amylose and the outer surface of HNT, when amylose helix wrapped around HNTs. The obtained amylose-HNTs can potentially be used as biosorbents for heavy metal ions (Wang et al., 2010) and dyes (Luo et al., 2010; Zhao & Liu, 2008), biomedical applications (Krejcova & Rabiskova, 2008), biological nanoreactors (Shchukin et al., 2005) and nano-fillers in biopolymer matrix (Xie et al., 2011).

References

Alpatova, A. L., Shan, W. Q., Babica, P., Upham, B. L., Rogensues, A. R., Masten, S. J., et al. (2010). Single-walled carbon nanotubes dispersed in aqueous media via non-covalent functionalization: Effect of dispersant on the stability, cytotoxicity, and epigenetic toxicity of nanotube suspensions. *Water Research*, *44*, 505–520.

Bandyopadhyaya, R., Nativ-Roth, E., Regev, O., & Yerushalmi-Rozen, R. (2002). Stabilization of individual carbon nanotubes in aqueous solutions. *Nano Letters*, *2*, 25–28.

Chang, P. R., Jian, R. J., Yu, J. G., & Ma, X. F. (2010). Fabrication and characterization of chitosan nanoparticles/plasticized-starch composites. *Food Chemistry*, *120*, 736–740.

Enyashin, A. N., Gemming, S., & Seifert, G. (2007). DNA-wrapped carbon nanotubes. *Nanotechnology*, *18*, 245702.

Karajanagi, S. S., Yang, H. C., Asuri, P., Sellitto, E., Dordick, J. S., & Kane, R. S. (2006). Protein-assisted solubilization of singlewalled carbon nanotubes. *Langmuir*, *22*, 1392–1395.

Kim, O. K., Je, J., Baldwin, J. W., Kooi, S., Pehrsson, P. E., & Buckley, L. J. (2004). Solubilization of single-wall carbon nanotubes by supramolecular encapsulation of helical amylose. *Journal of American Chemical Society*, *125*, 4426–4427.

Krejcova, K., & Rabiskova, M. (2008). Nano- and microtubes for drugs. *Chemicke Listy*, *102*, 35–39.

Luo, P., Zhao, Y. F., Zhang, B., Liu, J. D., Yang, Y., & Liu, J. F. (2010). Study on the adsorption of Neutral Red from aqueous solution onto halloysite nanotubes. *Water Research*, *44*, 1489–1497.

Ma, X. F., Chang, P. R., Yang, J. W., & Yu, J. G. (2009). Preparation and properties of glycerol plasticized-pea starch/zinc oxide-starch bionanocomposites. *Carbohydrate Polymers*, *75*, 472–478.

Nicolini, K. P., Fukamachi, C. R. B., Wypych, F., & Mangrich, A. S. (2009). Dehydrated halloysite intercalated mechanochemically with urea: Thermal behavior and structural aspects. *Journal of Colloid and Interface Science*, *338*, 474–479.

Peng, Y., Peter, D. S., Zongwen, L., Malcolm, E. R., Green, J., & Kepert, J. C. (2008). Functionalization of halloysite clay nanotubes by grafting with γ-minopropyltriethoxysilane. *The Journal of Physical Chemistry C*, *112*, 15742–15751.

Schoch, T. J. (1942). Fractionation of starch by selective precipitation with butanol. *Journal of American Chemical Society*, *64*, 2957–2961.

Shamsi, M. H., & Geckeler, K. E. (2008). The first biopolymer-wrapped non-carbon nanotubes. *Nanotechnology*, *19*, 075604.

Shchukin, D. G., Sukhorukov, G. B., Price, R. R., & Lvov, Y. M. (2005). Halloysite nanotubes as biomimetic nanoreactors. *Small*, *1*, 510–513.

Star, A., Steuerman, D. W., Heath, J. R., & Stoddart, J. F. (2002). Starched carbon nanotubes. *Angewandte Chemie International Edition*, *41*, 2508–2512.

Tierrablanca, E., Romero-García, J., Roman, P., & Cruz-Silva, R. (2010). Biomimetic polymerization of aniline using hematin supported on halloysite nanotubes. *Applied Catalysis A: General*, *381*, 267–273.

Wang, J. H., Zhang, X., Zhang, B., Zhao, Y. F., Zhai, R., Liu, J. D., et al. (2010). Rapid adsorption of Cr (VI) on modified halloysite nanotubes. *Desalination*, *259*, 22–28.

Xie, Y. F., Chang, P. R., Wang, S. J., Yu, J. G., & Ma, X. F. (2011). Preparation and properties of halloysite nanotubes/plasticized Dioscorea opposite Thunb. starch composites. *Carbohydrate Polymers*, *83*, 186–191.

Zhao, M. F., & Liu, P. (2008). Adsorption behavior of methylene blue on halloysite nanotubes. *Microporous and Mesoporous Materials*, *112*, 419–424.